

# TESLA cavity modeling and digital implementation with FPGA technology solution for control system development

Tomasz Czarski, Krzysztof Pozniak, Ryszard Romaniuk,  
ELHEP Laboratory, ISE, Warsaw University of Technology  
Stefan Simrock  
TESLA, DESY, Hamburg

## ABSTRACT

The cavity resonator modeling for the TESLA - TeV-Energy Superconducting Linear Accelerator project is initially introduced. The electromechanical model including Lorentz force detuning and beam loading is applied for analyzing the basic features of the plant. The continuous SIMULINK and digital MATLAB model implementation is developed as a reference for the hardware simulator based on the FPGA – Field Programmable Gate Array technology. The step operation mode has been applied for testing of the FPGA device coupled to the software control block. The FPGA signal processing has been verified according to the desired model of the real cavity plant. The numerical aspects have been investigated for the efficient design. Some experimental results have been presented for different cavity operational conditions. The following considerations have lead to the synthesis of the efficient algorithm for the cavity model, then implemented in the FPGA system.



**Keywords:** Super conducting cavity control, control theory, FPGA, DSP, VHDL, system simulation.

## 1. INTRODUCTION

The authors have recently studied the control problem, presented in this paper, in a series of previous documents, included in the references. The mentioned work concerns a modeling development of the TESLA cavity for the LLRF - Low Level Radio Frequency control system. The first part of the current paper attempts to order and recapitulate the achieved results in the concise manner. Consequently, the second part of the paper, presents some new results leading to the synthesis of the digital algorithm efficiently implemented in the FPGA system. Therefore, the paper establishes a self-contained design report from an abstract consideration to the final practical result.

The TESLA project is based on the nine-cell super conducting niobium resonators to accelerate electrons and positrons. The acceleration structure is operated in standing  $\pi$ -mode wave at the frequency of 1,3 GHz. The RF oscillating field is synchronized with the motion of a particle moving at the velocity of light across the cavity (figure1).

The LLRF cavity control system for the TESLA project has been developed to stabilize the accelerating fields of the resonators. The control section, powered by one klystron, consists of four cryomodules containing eight cavities each. One klystron supplies the RF power of 10 MW to 32 cavities through the coupled wave-guide with a circulator. The cavities are driven with the pulses of 1.3 ms duration and the average accelerating gradients of 25 MV/m. The control feedback system regulates the vector sum of the pulsed accelerating fields in multiple cavities. The fast amplitude and phase control of the cavity field is accomplished by modulation of the signal driving the klystron. The cavity RF signal is down-converted to an intermediate frequency of 250 KHz preserving the amplitude and phase information. The ADC and DAC converters link the analog and digital parts of the system. The digital signal processing is applied for the field vector detection and filtering. The digital controller stabilizes the detected real (in-phase) and imaginary (quadrature) components of the incident wave according to the desired set point. Additionally, the adaptive feed-forward is applied to improve compensation of repetitive perturbations induced by the beam loading and by the dynamic Lorentz force detuning (figure 1).

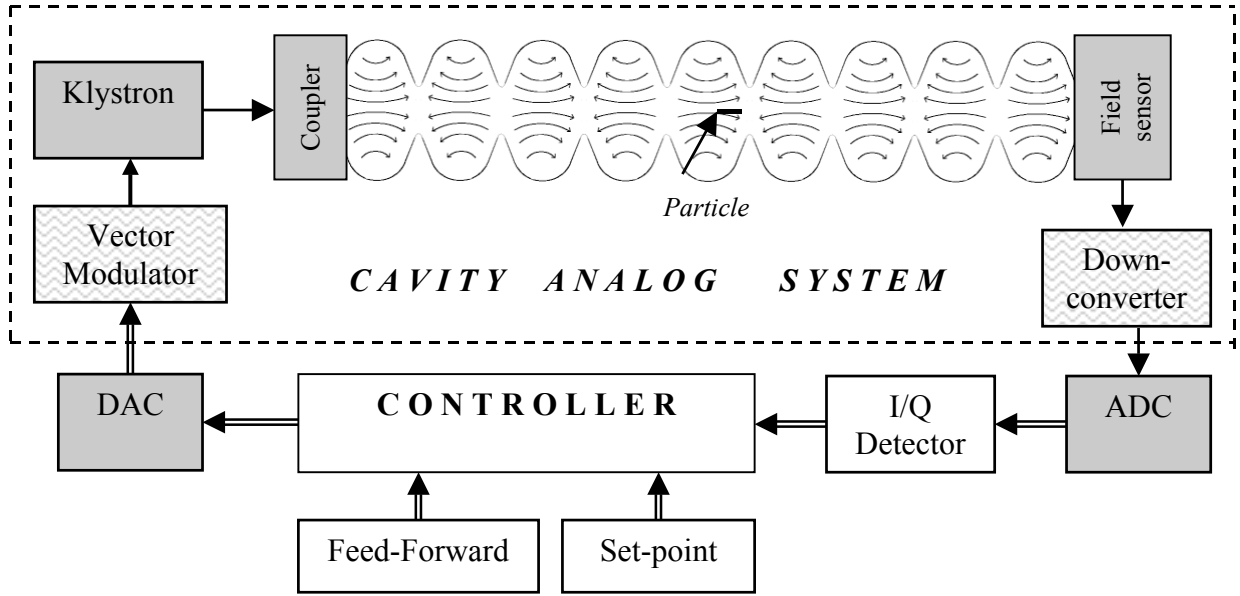


Figure 1. Cavity environment and simplified block diagram of cavity control system.

The cavity resonator modeling has been developed for the efficient testing of the control system and for the investigation of the optimal control method. The software models allow testing of the hardware controller by the step operation mode. The FPGA hardware implementation of the cavity model is intended for the real time operation.

## 2. OUTLOOK OF CAVITY MODELING

### 2.1 Electrical circuit modeling

The equivalent representations of the chain of nine cells of the resonator are magnetically coupled resonant circuits. The following simplified considerations are limited to one cavity represented as a single LCR circuit coupled to the wave-guide driven by the klystron. This simple version is quite sufficient for the purpose of the cavity control modeling. The simplified circuit model for the cavity environment is presented in figure 2. All the current ( $J$ ) and voltage ( $U$ ) quantities are represented in the *Laplace space*.

The RF current generator  $J_k$ , driving the wave-guide with circulator, models the klystron as a power amplifier. The wave-guide, as a transmission line, is parameterized by the characteristic impedance  $Z_0$  and time delay  $T_w$ . The cavity is represented as the resonant LCR circuit with impedance  $Z_c$  coupled to the wave-guide. The beam loading can be modeled as a current sink  $J_b$  fed by the electromagnetic field of the cavity. The bunched beam current has typical  $\sim 2$  ps pulse duration, 1 MHz rate and an average value of 8 mA.

The *forward wave*, represented by voltage  $U_f$  and current  $J_f$ , drives the coupler, which converts the signals according to the transformation ratio  $1:N$ . Superposition of the output coupler signals (represented by voltage  $U_2$  and current  $J_2$ ) and the beam loading results in the cavity current  $J_c$  and, related by impedance  $Z_c$ , cavity voltage  $U_c$ . The *reflected wave* (represented by voltage  $U_r$  and current  $J_r$ ) is isolated from the klystron output and dissipates in the circulator load, matched to the wave-guide.

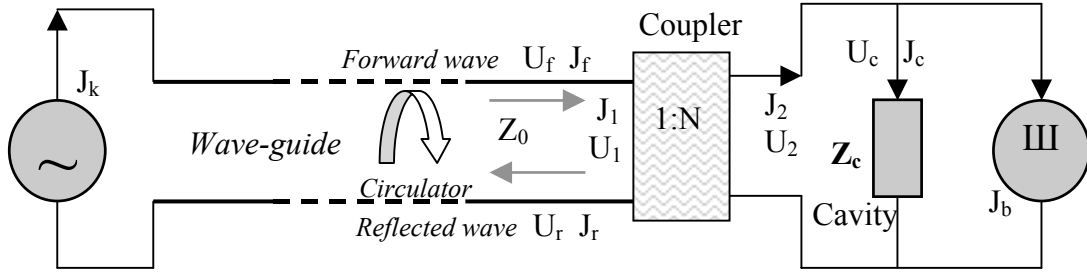


Figure 2. Circuit model of cavity environment.

Applying an equivalent parallel resistance connection  $R_L \equiv N^2 Z_0 \parallel R$ ,  
and the cavity loaded impedance  $Z_L = (1/R_L + sC + 1/sL)^{-1}$ ,  
and substituting the generator current  $J_g \equiv J_f/N$ ,  
results in the cavity voltage  $U_c = Z_L \cdot (2J_g - J_b) = Z_L \cdot J$ .

Therefore, the cavity loaded impedance  $Z_L(s)$  can be represented by the transfer function in the corresponding forms:

$$Z_L(s) = (1/R_L + sC + 1/sL)^{-1} = \omega_0 \cdot \rho s / (s\omega_0/Q_L + s^2 + \omega_0^2) = \omega_{1/2} \cdot R_L / (\omega_{1/2} + (s^2 + \omega_0^2)/2s),$$

where, the following *secondary* parameters (derived from the *primary* LRC parameters) are applied:

resonance frequency  $\omega_0 = 2\pi f_0 = (LC)^{-1/2}$ ,  
characteristic resistance  $\rho = (L/C)^{1/2}$ ,  
shunt impedance  $R_L \equiv R \parallel N^2 \cdot Z_0$ ,  
loaded quality factor  $Q_L = R_L/\rho$ ,  
half-bandwidth (HWHM)  $\omega_{1/2} = 2\pi f_{1/2} = 1/2CR_L = \omega_0/2Q_L$ .

According to the stability of the RF generator pulsation  $\omega_g$  and due to a narrow resonator bandwidth, the cavity voltage can be modeled in *time domain* as an *analytical signal* represented as a vector or phasor in the complex domain:

$$\mathbf{u}(t) \equiv [u_r, u_i] \equiv u_r + i u_i = a(t) \cdot \cos(\omega_g t + \varphi(t)) + i \sin(\omega_g t + \varphi(t)) = a(t) \cdot \exp(i \cdot (\omega_g t + \varphi(t))),$$

where,  $u_r, u_i$  – are the real and imaginary components of the RF oscillation; the amplitude  $a(t)$  and the phase  $\varphi(t)$  are slowly time-varying parameters relatively to the period of the RF signal carrier.

The cavity current is modeled as an *analytical signal*  $\mathbf{j}(t) = 2\mathbf{j}_g(t) - \mathbf{j}_b(t)$ , where  $\mathbf{j}_b$  corresponds to  $\omega_g$  Fourier component of the beam loading current. The relation between the current and the voltage is given in the *Laplace space*:

$$\mathbf{U}(s) = Z_L(s) \cdot \mathbf{J}(s),$$

where,  $\mathbf{U}(s)$  and  $\mathbf{J}(s) = 2\mathbf{J}_g(s) - \mathbf{J}_b(s)$ , are the Laplace transforms of the *analytical signal* for the voltage and current respectively.

Alternative, more useful representation of the cavity signal in *time domain* is *complex envelope* derived by the complex demodulation (down conversion) of the *analytical signal* which applies the operator  $\exp(-i\omega_g t)$  for the given pulsation  $\omega_g$ . *Vice versa*, the complex modulation (up conversion) of the *envelope* applies the operator  $\exp(i\omega_g t)$  and yields the *analytical signal* for the given pulsation  $\omega_g$ . The *complex envelope* for the cavity current  $\mathbf{i}(t)$  and voltage  $\mathbf{v}(t)$  can be represented as a vector or phasor by its real I - in-phase, and imaginary Q - quadrature components as follows (for the voltage case):

$$(I, Q)_{\text{voltage}} \equiv \mathbf{v}(t) \equiv [v_r, v_i] \equiv v_r + i v_i \equiv \mathbf{u}(t) \cdot \exp(-i\omega_g t) = a(t) e^{i\varphi(t)} \equiv [a(t) \cos \varphi(t), a(t) \sin \varphi(t)].$$

The comprehensive signal relation is modeled by the signal-flow graph according to figure 3.

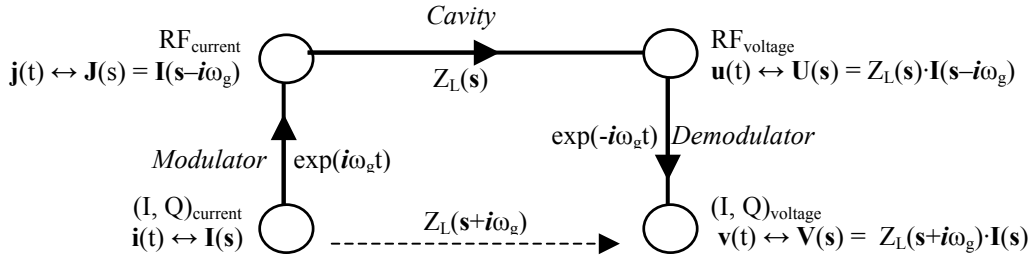


Figure 3. Cavity signal-flow graph for *complex envelope* and *analytical signal*.

The successive operations, presented by the signal-flow graph in figure 3, yield the direct relation between the cavity input and output *complex envelope* in the *Laplace space* as follows:

$$\mathbf{V}(\mathbf{s}) = Z_L(\mathbf{s} + i\omega_g) \cdot \mathbf{I}(\mathbf{s}),$$

where,  $\mathbf{V}(\mathbf{s})$  and  $\mathbf{I}(\mathbf{s}) = 2\mathbf{I}_g(\mathbf{s}) - \mathbf{I}_b(\mathbf{s})$ , are the Laplace transforms of the *complex envelope* for the voltage and the current respectively.

Thus, the resultant cavity transfer function is transformed to the low-pass filter. The analytical form of the impedance can be effectively simplified for signals with a narrow spectral range relative to the generator frequency close to the cavity resonance pulsation, then for  $|\mathbf{s}| \ll \omega_g \approx \omega_0$  yields:

$$Z_L(\mathbf{s} + i\omega_g) \approx \omega_{1/2} \cdot R_L / (\mathbf{s} + \omega_{1/2} - i\Delta\omega),$$

where, cavity detuning is  $2\pi\Delta f = \Delta\omega \equiv \omega_0 - \omega_g$ .

Therefore, the *complex envelope* relation for the cavity signals can be written in the *Laplace space* as follows:

$$(\mathbf{s} + \omega_{1/2} - i\Delta\omega) \cdot \mathbf{V}(\mathbf{s}) = \omega_{1/2} \cdot R_L \cdot \mathbf{I}(\mathbf{s}).$$

Moving to the *time domain* yields the *state space* equation with  $\mathbf{v}(t)$  as a state vector of the cavity electrical model:

$$d\mathbf{v}(t)/dt = \mathbf{A}_e \cdot \mathbf{v}(t) + \omega_{1/2} \cdot R_L \cdot \mathbf{i}(t)$$

where,  $\mathbf{v}(t)$  and  $\mathbf{i}(t) = 2\mathbf{i}_g(t) - \mathbf{i}_b(t)$  are the time dependent *complex envelope* for the voltage and current respectively and phasor  $\mathbf{A}_e = -\omega_{1/2} + i\Delta\omega$  for the complex representation or matrix  $\mathbf{A}_e = [-\omega_{1/2}, -\Delta\omega; \Delta\omega, -\omega_{1/2}]$  for the vector representation (according to the MATLAB description).

Thus, the resultant *state space* equation for the *complex envelope* depends on the cavity bandwidth and detuning only. The simplified relationship for the cavity *envelope* allows for the control system modeling within the low-level frequency range.

## 2.2. Electromechanical modeling.

The super-conducting resonator has an extremely high loaded quality factor  $Q_L \sim 3 \cdot 10^6$  and the narrow bandwidth of about 430 Hz (FWHM). Hence, the cavity is very sensitive to the mechanical distortion caused by microphonics and the Lorentz force, changing the resonator's frequency. Due to the Lorentz force, the cavity resonance frequency changes with the rising field gradient. The mechanical model of the super-conductive cavity describes the Lorentz force detuning, which is a function of the square of time varying field gradient. It is based on the heuristic relationship for the independent mechanical modes of the cavity with the resonance frequency  $f_m$  and the mechanical quality factor  $Q_m$  for the given mode. Each of the mechanical modes is driven by square of the cavity field gradient  $v^2$  according to the equation, as follows:

$$d\alpha_m(t)/dt + 2\pi f_m \cdot \alpha_m(t)/Q_m + (2\pi f_m)^2 \cdot \Delta\omega_m(t) = - (2\pi f_m)^2 \cdot 2\pi \cdot K_m \cdot v^2(t) \quad \text{with} \quad \alpha_m(t) = d(\Delta\omega_m(t))/dt,$$

where, the time-varying detuning  $\Delta\omega_m(t)$  and its time derivative  $\alpha_m(t)$  are two state-variables for the m-th mode, and parameter  $K_m$  is the Lorentz force detuning constant.

Applying the *vector-matrix* format of the *state space* equation for the m-th mechanical mode yields:

$$d\mathbf{w}_m(t)/dt = \mathbf{A}_m \cdot \mathbf{w}_m(t) + \mathbf{B}_m \cdot v^2(t), \quad \text{where,}$$

state vector  $\mathbf{w}_m(t) = [\Delta\omega_m(t); \alpha_m(t)]$ , system matrix  $\mathbf{A}_m = [0, 1; -(2\pi f_m)^2, -2\pi f_m/Q_m]$ ,  
input matrix  $\mathbf{B}_m = [0; -(2\pi f_m)^2 \cdot K_m]$ , square of the cavity gradient =  $v^2(t)$ .

The resultant cavity detuning is  $\Delta\omega(t) = \sum \Delta\omega_m(t) + \Delta\omega_0$ , where  $\Delta\omega_0$  – initial *predetuning*. The initial *predetuning* is a mechanically biased component, which attempts to compensate the EM forced detuning factor, during operational condition of the cavity.

Three dominating resonance frequencies are considered in the cavity model presented below and the superposition of all modes yield the resultant detuning.

### 2.3 SIMULINK modeling.

The continuous model of the cavity is composed applying the SIMULINK – dynamic system simulation for MATLAB according to figure 4.

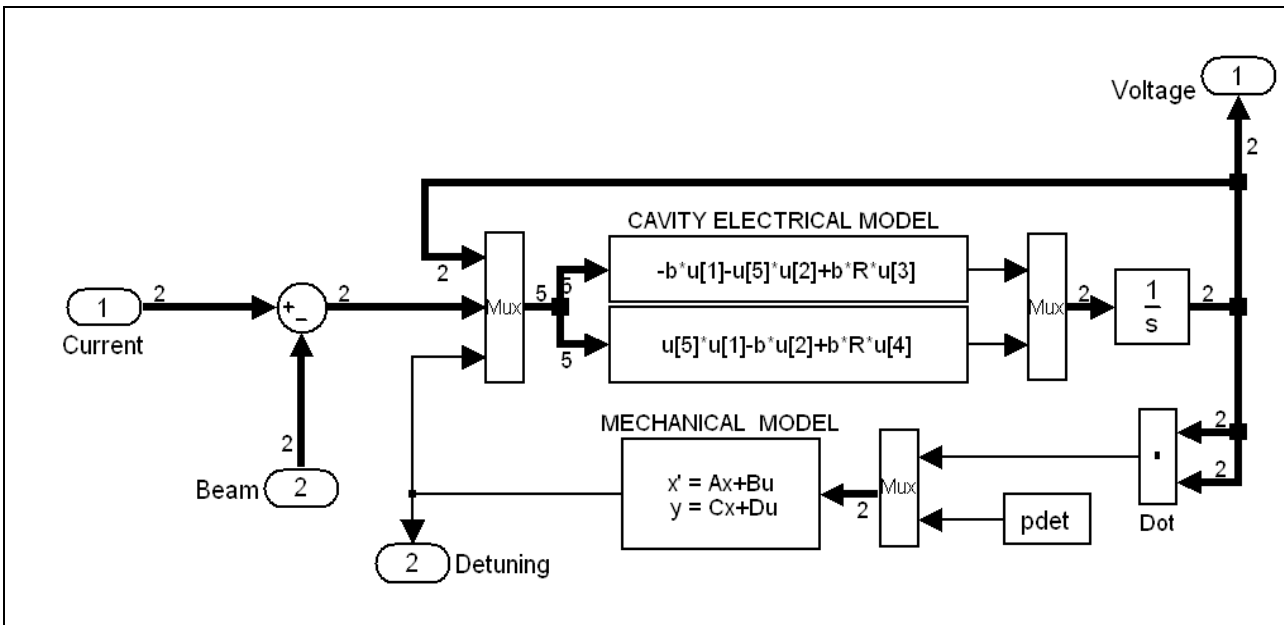


Figure 4. Cavity SIMULINK model.

The electrical part of the cavity model consists of the arithmetical function block driven by the current generator and the beam loading. The integrator output feeds the input according to the *state-variables* relation. Additionally, the non-stationary detuning modulates the object feature. The square of the cavity field gradient drives the mechanical part of the model resulting in the Lorentz force-detuning component for each mode. The multi-mode *state space* block puts the detuning together with the initial *predetuning* as a superposition of all modes.

The comprehensive model of the cavity control system has been developed in the SIMULINK Toolbox to investigate different operational conditions (figure 5). The system operates as a continuous model with fixed micro step of 0.1  $\mu$ s duration. The *control block* subsystem generates signals of the beam, feed-forward, set point and gain according to the system requirements. Additionally, it applies the information of the cavity detuning. The proportional controller amplifies the error signal and closes the feedback loop. The transducers match properly signals level of the cavity subsystem to the controller circuit. The *channel distortion* simulates the amplitude attenuation and phase shifting of the transmission line. The intermediate frequency modulator converts the cavity output vector to the signal of frequency 250 kHz. Therefore, the data samples, like from the down-converter, can be conveyed to the outer digital controller.

The cavity model can be driven by the SIMULINK controller or by the outer one applying the Matlab workspace data. In the latter case, the constant  $I_Q$  vector drives the cavity during simulation step of the process, and all resulting data are sent to the Matlab *workspace*.

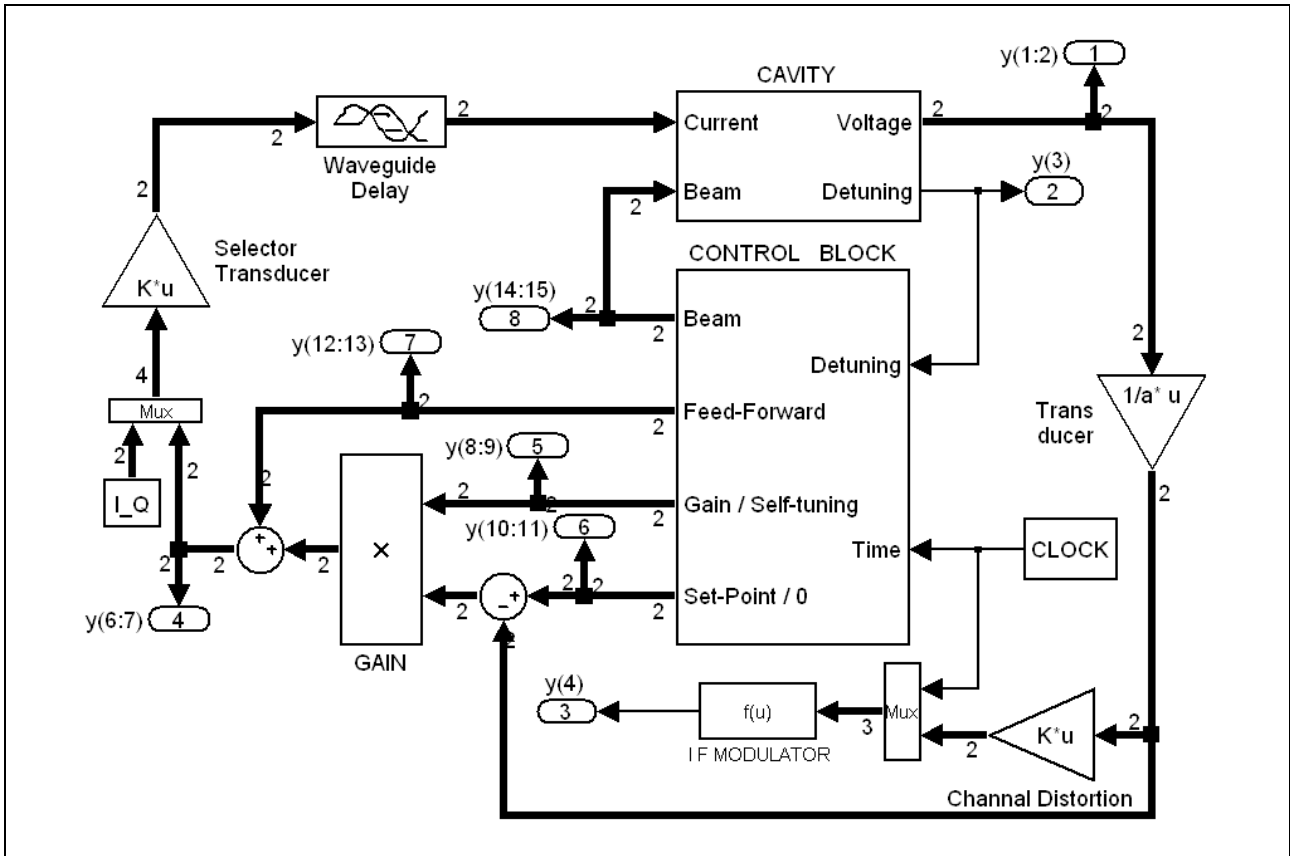


Figure 5. Cavity control system SIMULINK model.

The main parameters of the model, for simulation examples, are available from the MATLAB file and are combined in the table below.

CAVITY ELECTRICAL parameters	CAVITY MECHANICAL modes parameters
$f_0 = 1300$ .....resonance frequency [MHz]	$\mathbf{f} = [280, 340, 420]$ .....resonance frequencies vector [Hz]
$\rho = 520$ .....characteristic resistance [ $\Omega$ ]	
$Q_L = 3 \cdot 10^6$ .....loaded quality factor	$\mathbf{Q} = [100, 100, 100]$ ..... quality factors vector
$R_L = Q_L \cdot \rho = 1560$ .....load resistance [M $\Omega$ ]	
$f_{1/2} = f_0 / 2Q_L = 216$ .....half band-width [Hz]	$\mathbf{K} = [0.4, 0.3, 0.2]$ ..... Lorentz force detuning constants vector [Hz/(MV) <sup>2</sup> ]
$\Delta f = 431$ .....pre-detuning [Hz]	

The step response of the cavity model is considered as a reference performance for the comparison of different implementations of the cavity signal processing algorithm. The step response of the pure electrical model with steady detuning, for different values of the cavity detuning, illustrates figure 6.

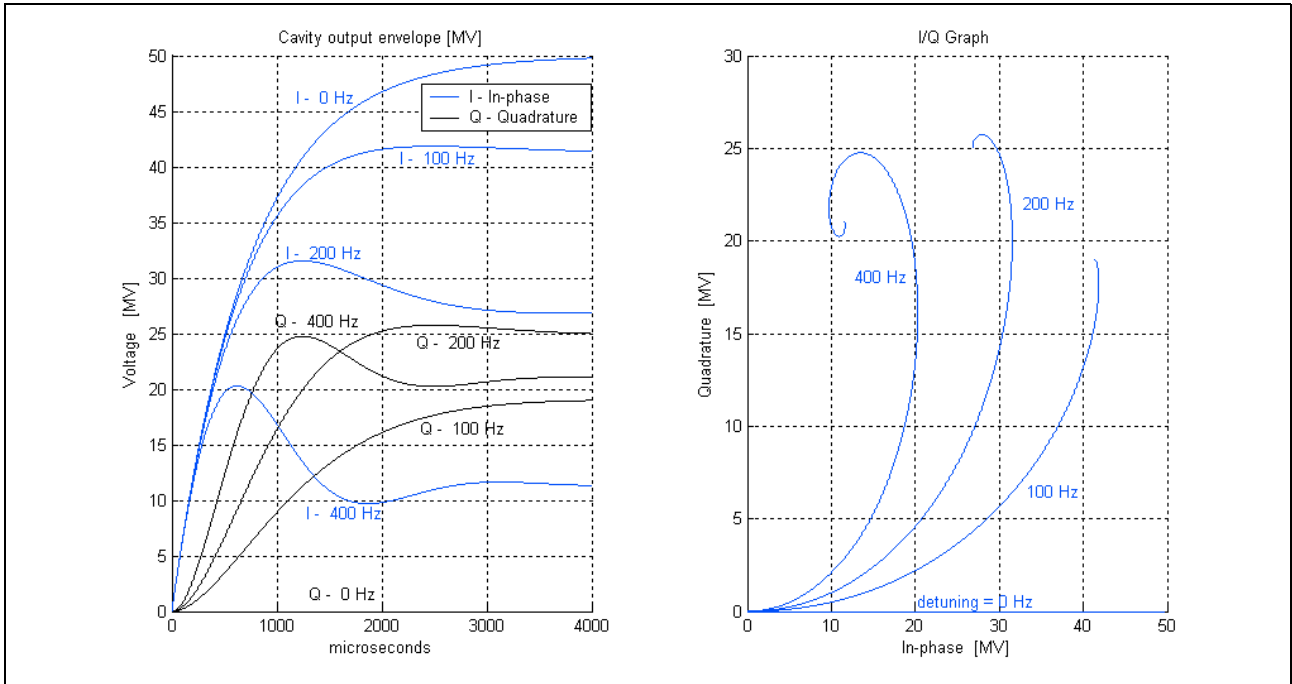


Figure 6. Step response of cavity electrical model for driving current of  $i_g = 16$  mA for different detuning.

The pure mechanical model is weakly damped. But one can excite dynamic ponderomotive instability for the sufficiently high field gradient for the resultant electromechanical model of the cavity (figure 7).

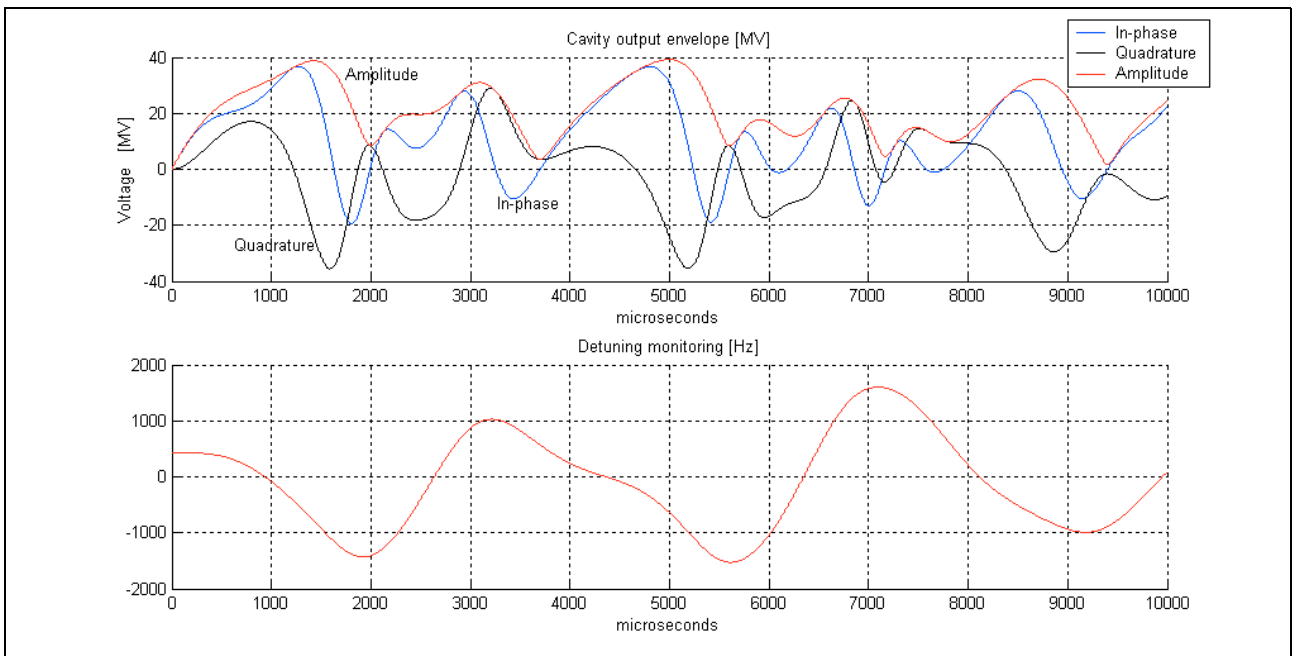


Figure 7. Step response of cavity electromechanical model for driving current of  $i_g = 16$  mA.

### 3. DIGITAL IMPLEMENTATION OF CAVITY MODEL

#### 3.1 MATLAB implementation of cavity model

The discrete processing of the cavity algorithm has been developed for digital implementation of the cavity model. The continuous model of the cavity behavior can be estimated by the arithmetic procedure realized iteratively in the finite number of steps.

The continuous *state-space* model is presented for the electrical and mechanical parts, respectively:

$$\begin{aligned} d\mathbf{v}(t)/dt &= \mathbf{A}_e \cdot \mathbf{v}(t) + \omega_{1/2} \cdot R_L \cdot \mathbf{i}(t), \quad \text{where } \mathbf{i}(t) = 2\mathbf{i}_g(t) - \mathbf{i}_b(t), \\ d\mathbf{w}_m(t)/dt &= \mathbf{A}_m \cdot \mathbf{w}_m(t) + \mathbf{B}_m \cdot v^2(t). \end{aligned}$$

Applying the Euler approximation (or the Matlab discretization) for the time derivative of a general variable  $x$ :  $dx/dt \approx (x_n - x_{n-1})/T$ , for successive (n-1)-th and n-th samples, with time interval of  $T$ , and with identity matrix  $\mathbf{I}$ , yields the recursive equations:

$$\begin{aligned} \text{for the electrical model} \quad \mathbf{v}_n &= (\mathbf{I} + T \cdot \mathbf{A}_e) \cdot \mathbf{v}_{n-1} + T \cdot \omega_{1/2} \cdot R_L \cdot \mathbf{i}_n, \quad \text{where } \mathbf{i}_n = 2(\mathbf{i}_g)_n - (\mathbf{i}_b)_n, \\ \text{for the mechanical m-th mode} \quad (\mathbf{w}_m)_n &= (\mathbf{I} + T \cdot \mathbf{A}_m) \cdot (\mathbf{w}_m)_{n-1} + T \cdot \mathbf{B}_m \cdot v_n^2. \end{aligned}$$

Applying the MATLAB notation, with omitting time indexes and providing new symbols, yields:

$$\text{for the electrical model:} \quad \mathbf{v} = \mathbf{E} \cdot \mathbf{v} + \mathbf{v}0 - \text{Beam},$$

where, discrete system matrix  $\mathbf{E} = [1 - T \cdot \omega_{1/2}, -T \cdot \Delta\omega; T \cdot \Delta\omega, 1 - T \cdot \omega_{1/2}]$  and unified input signals  $\mathbf{v}0 = T \cdot \omega_{1/2} \cdot R_L \cdot 2(\mathbf{i}_g)_n$  for the current generator, and  $\text{Beam} = T \cdot \omega_{1/2} \cdot R_L \cdot (\mathbf{i}_b)_n$ , for the beam loading:

$$\text{for m-th mechanical mode:} \quad \mathbf{w}_m = (\mathbf{I} + T \cdot \mathbf{A}_m) \cdot \mathbf{w}_m + T \cdot \mathbf{B}_m \cdot v^2.$$

Applying the common state vector  $\mathbf{w}$  and discrete matrix  $\mathbf{A}$  and  $\mathbf{B}$ , for the resultant mechanical model, yields:

$$\mathbf{w} = \mathbf{A} \cdot \mathbf{w} + \mathbf{B} \cdot v^2,$$

where, partial state vector for m-th mode:  $\mathbf{w}(2m-1:2m) = \mathbf{w}_m$ ,

partial system matrix for m-th mode:  $\mathbf{A}(2m-1:2m, 2m-1:2m) = [1, T; -T \cdot (2\pi f_m)^2, 1 - 2\pi f_m \cdot T / Q_m]$ ,

partial input matrix for m-th mode:  $\mathbf{B}(2m-1:2m) = [0; -T \cdot (2\pi f_m)^2 \cdot K_m]$ ,

The resultant detuning of the cavity is  $\Delta\omega = \sum \mathbf{w}(2m-1) + w0$ , where  $w0$  – initial *predetuning*.

The discrete cavity algorithm, for the parallel electrical and mechanical iterative processing, has been implemented applying MATLAB code with time interval  $T = 1 \mu\text{s}$ , according to the schematic diagram presented in figure 8.

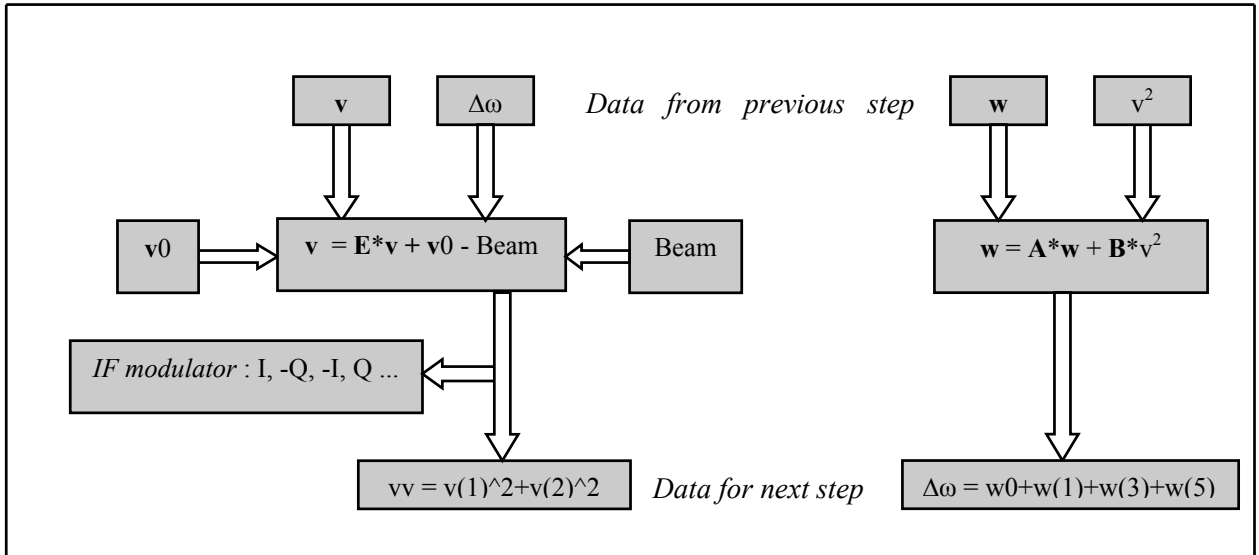


Figure 8. Schematic diagram of discrete processing for one step of cavity algorithm.

### 3.2 DSP modeling and numerical optimization.

The hardware implementation of the cavity discrete model requires the numerical care due to the integer processing and limited resolution of the parameters and variables values involved in the digital signal processing (DSP). The proper scaling procedure may provide the top potential precision by utilizing the full range for every operation what can be compared to the floating-point arithmetic. The main arithmetic processing, for each variable  $x_i$ , is a linear combination of the corresponding variables  $x_k$ , with parameter  $a_{ik}$ , for every step of the algorithm, as follows:

$$x_i = \sum_{\kappa} \alpha_{ik} * x_k .$$

The three stages of the algorithm synthesis, for the DSP modeling, are distinguished in the following considerations.

1. The preliminary scaling, with change of the parameters and variables, simplifies the equations and unifies the factors. The *primary* range of the parameters extends up to  $10^7$  for the raw algorithm.

2. The best numerical accuracy can be achieved for the advanced scaling maximizing the fractional values within the given *secondary* range and common for all the partial values. After multiplication, the gained product should be rescaled to preserve its proper value. The most appropriate values for scaling coefficients are the power of two, for the binary arithmetic. Thus, the resultant equation term  $R_{ik}$  as a product of three factors is as follows:

$$R_{ik} = A_{ik} \cdot X_k / S_{ik},$$

where, scaled parameter  $A_{ik} = s_{ik} \cdot a_{ik}$ , scaled variable  $X_k = s_k \cdot x_k$ , rescaling coefficient  $S_{ik} = s_{ik} \cdot s_k / s_i$ ,

$s_{ik}$  – scaling factor for parameter  $a_{ik}$ ,  $s_k$  – scaling factor for variable  $x_k$ ,  $s_i$  – scaling factor for variable  $x_i$ .

Consequently, the scaled parameters and maximum values of the variables may be contracted within one-decade range only. The values of the parameters and variables have been matched to the *secondary* real range (-64, +64) corresponding to the cavity envelope voltage [MV]. The step response of the modified discrete cavity model is shown in figure 9, for all scaled variables.

3. The modified discrete cavity model, with scaled parameters and variables, within the secondary real range (-64, +64), has been finally adapted to the features of the hardware implementation with the N-bit resolution. Therefore, the advanced, *integer* model of the cavity has been implemented in the MATLAB system for a given N-bit resolution. Consequently, the real range (-64, +64) has been extended to the integer one, applying a global scaling factor of  $J = 2^{(N-7)}$  for all parameters and variables of the cavity algorithm.

The numerical accuracy of the final *integer* model has been tested for the cavity envelope step response, for different bit resolutions, and diverse scaling factors. The modified discrete cavity model, with scaled parameters and variables within *secondary* real range (-64, +64), has been considered as a reference. The relative mean error of the envelope  $Err(N)$  for N-bit resolution, has been calculated according to the expression:

$$Err(N) = \sum |(V_N)_n - (V_{ref})_n| / \sum |(V_{ref})_n|,$$

where  $(V_{ref})_n$  – the sample of the reference envelope for n-th step,  $(V_N)_n$  – the sample of the N-bit resolution envelope for n-th step.

The experimental results are presented in figure 10 for chosen variables and parameters.

Two options of the resolution have been considered for the final FPGA realization and relative errors for the MATLAB *integer* model have been estimated respectively, as follows:

$Err(32) = 3.6532e-006$  - for 32-bit resolution, and  $Err(18) = 0.0533$ - for 18-bit resolution.

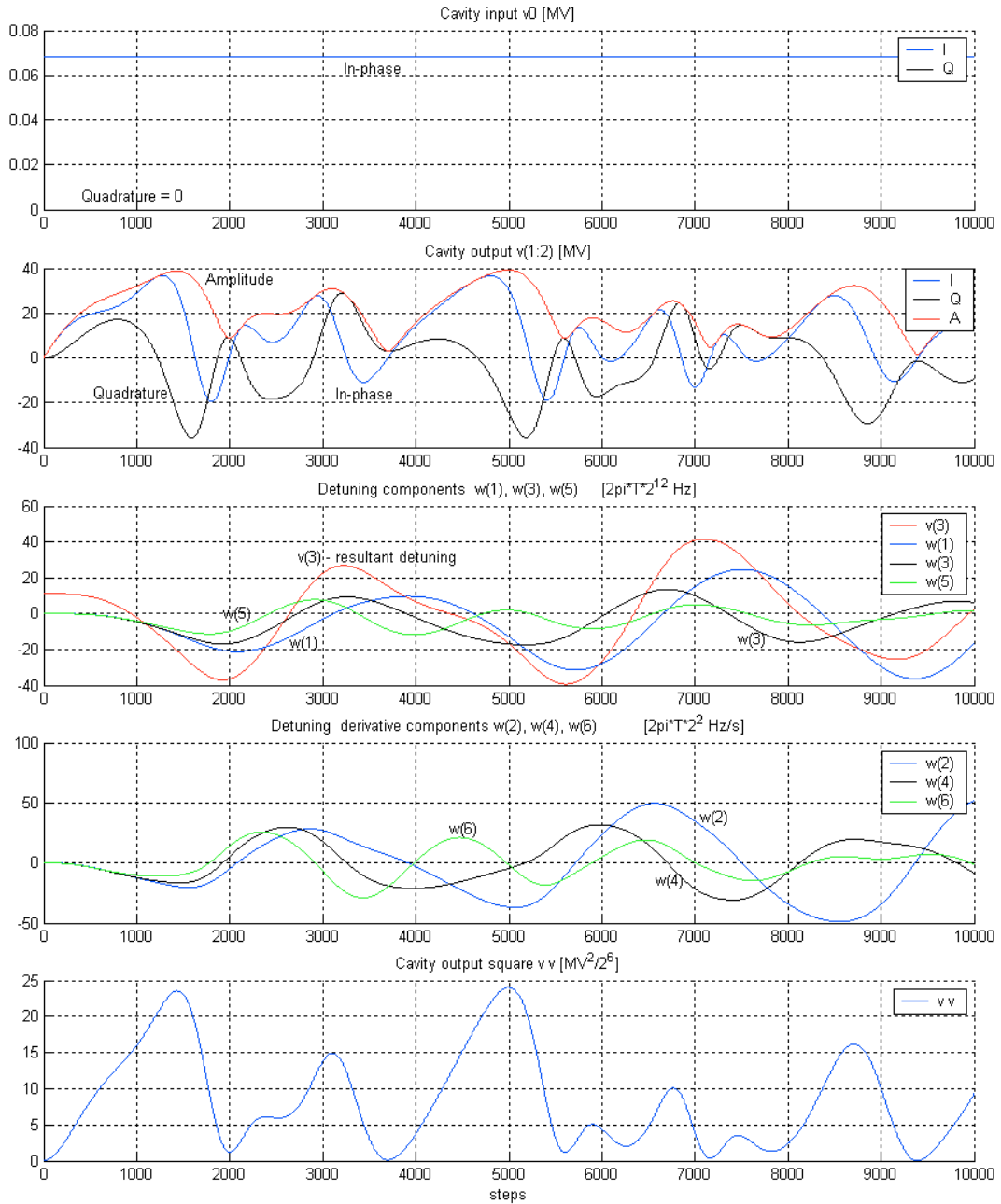


Figure 9. Step response for scaled variables of modified discrete cavity model.

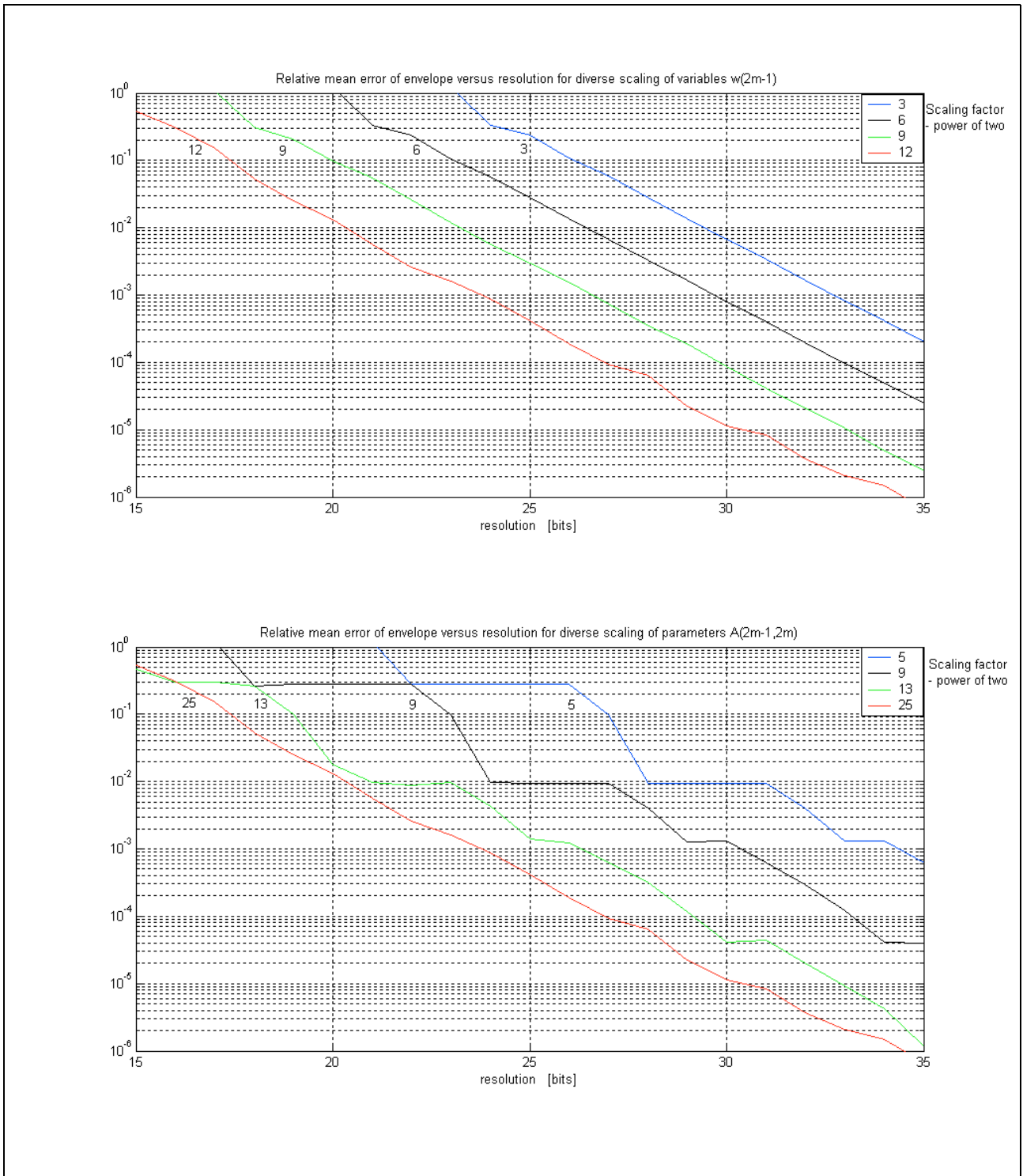


Figure 10. Relative mean error of envelope versus bit resolution for diverse scaling of chosen variables and parameters.

### 3.3 Cavity simulator based on FPGA technology.

The MATLAB, *integer* model of the cavity, with scaled parameters and variables, has been considered as the reference pattern for the hardware implementation.

The discrete algorithm, describing the cavity, was realized in the VHDL - Very\_High\_Speed\_Integrated\_Circuit\_Hardware\_Description\_Language. The algorithm has the form of a fully parameterized behavioral and self-contained description. This way assures a simple possibility to choose the resolution and the position for the fixed point. It is achieved by setting the proper parameters for the compilation process. The compiler automatically selects the logical and DSP resources and performs the optimization. For example, the 32-bit resolution of the cavity model with three mechanical modes requires 96 multipliers. The 18-bit resolution requires only 24 multiplying circuits.

To realize the processing, a synchronous pipeline bus was applied, clocked at 40MHz. The system flexibility, obtained in this way, gives the possibility to choose arbitrarily the number of clock periods necessary to do successive, partial calculations by the DSP blocks.

The application, which was practically used, and is described here, is performed during the time of eight 40MHz clock periods, this means in 200ns. The described implementation was realized for the VirtexII of 3000 series, with the use of "Leonardo Spectrum 2002d" compiler and XILINX ISE Integrated Environment.

The step operation mode has been applied for testing the FPGA device coupled to the MATLAB system via the communication interface. The FPGA signal processing has been verified according to the desired algorithm. Two adaptations of the cavity simulator: 32-bit and 18-bit resolution has been considered for the FPGA realization. The numerical accuracy of the FPGA cavity simulator has been estimated as follows:  $Err(32) = 7.5830e-006$  for the 32-bit resolution and  $Err(18) = 0.0532$  for the 18-bit resolution, in relation to the MATLAB scaled model of the full-resolution. The evaluation of the FPGA cavity simulator step responses is presented in figure 11 for these two performances.

The MATLAB *integer* model has been compared to the FPGA implementation of the equivalent resolution and mutual numerical errors have been estimated as follow:  $Err(32) = 8.1083e-006$  for 32-bit resolution and  $Err(18) = 9.0818e-4$  for 18-bit resolution.

The 18-bit resolution version of the FPGA cavity simulator is expected to be quite sufficient for the simulation purpose. The limited validity of the cavity mechanical model and 12-bit resolution of the preferred analog-to-digital converter do not require a resolution of better quality.

The simulation results of the step mode, for the real operational condition, are presented in figure 12 for the 18-bit resolution of the FPGA cavity simulator. In this case, the cavity is driven in the pulse mode forced by the control feedback supported by the feed-forward. During the first stage of the operation, the cavity is *filling* with constant forward power, resulting in an exponential increase of the electromagnetic field, according to its natural behavior, in the resonance condition. When the cavity gradient has reached half of the final value, (no reflection for ideal condition) the beam loading current is injected, resulting in the steady-state *flattop* operation. Turning off both, the generator and the beam current yields an exponential *decay* of the cavity field.

The main parameters of the FPGA simulator are combining in the table below.

DSP resolution	Equivalent output range	Maximum carrier frequency	Minimum Processing time	DAC and ADC Resolution
18 [bit]	$\pm 64$ [MV]	1.25 [MHz]	200 [ns]	14 [bit]

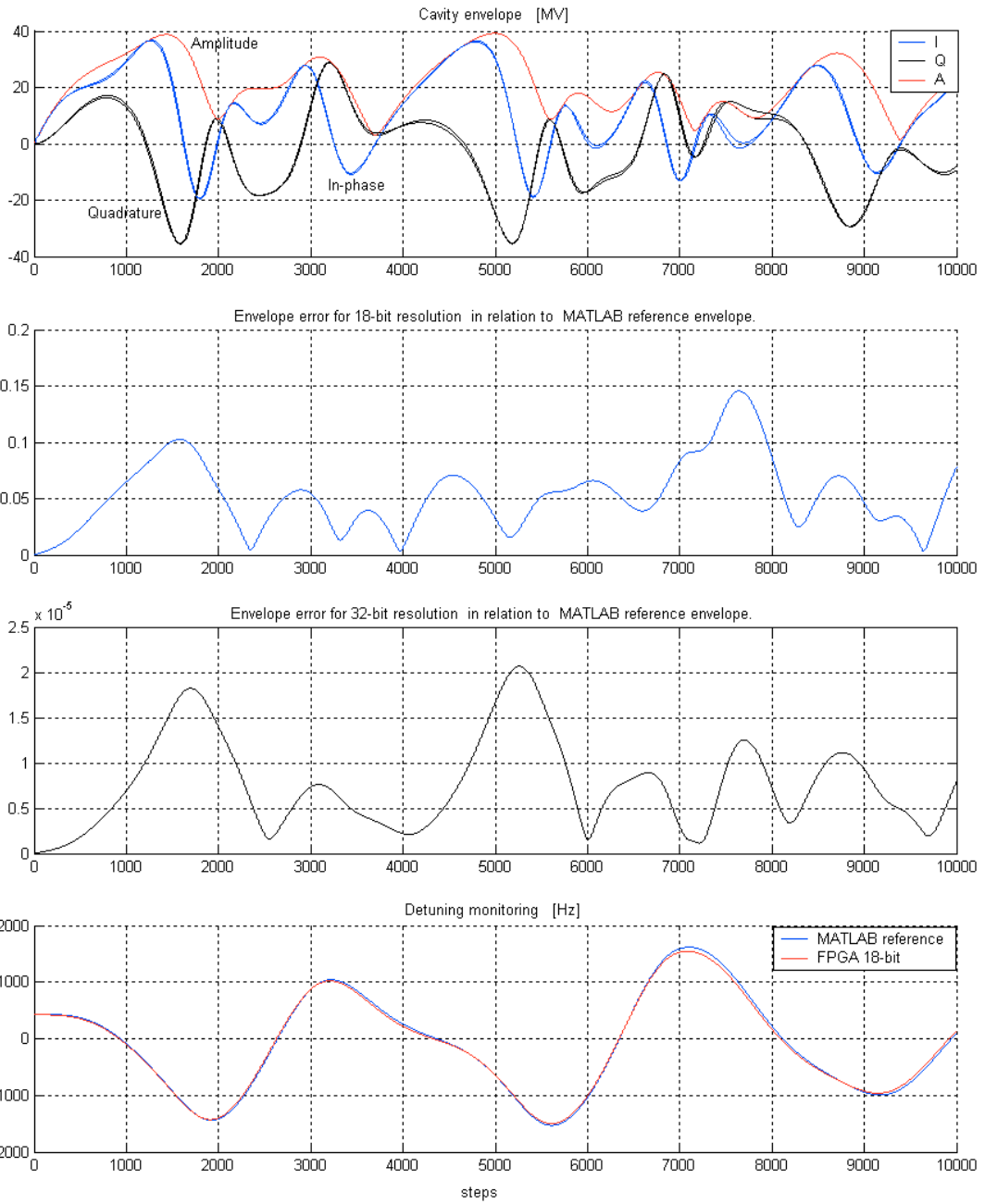


Figure 11. Step responses comparison for 32-bit and 18-bit resolution of FPGA cavity simulator implementation.

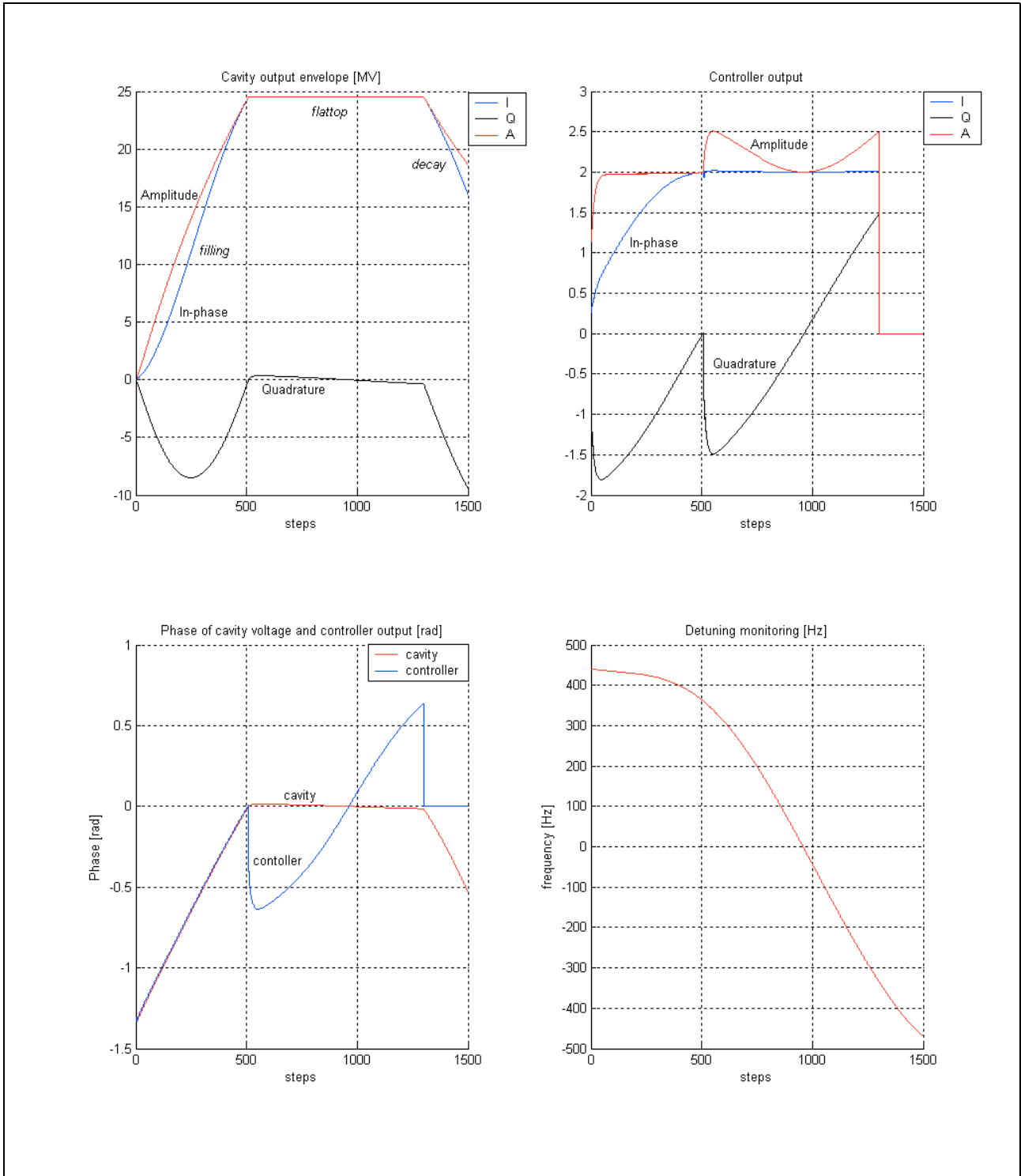


Figure 12. FPGA cavity and MATLAB controller output for real operation condition (average beam=8mA).

#### 4. REAL TIME TESTS

The real time tests have been carried out according to the schematic block diagram in figure 13. The FPGA controller drives the FPGA cavity simulator via internal digital connection (18-bit data resolution). The alternative connection with the MATLAB system allows for the step operation mode as well. The MATLAB system loads parameters and data to the FPGA memory tables before the simulation test. Subsequently the FPGA system can run itself cyclically according to the given data tables. The digital-to-analog converter (DAC) conveys data from the FPGA cavity simulator or from the FPGA controller to the oscilloscope. The simulation results, for the real operational condition, are presented in figures from 14 to 17. The cavity is driven in the pulse mode forced by the control feedback supported by the feed-forward.

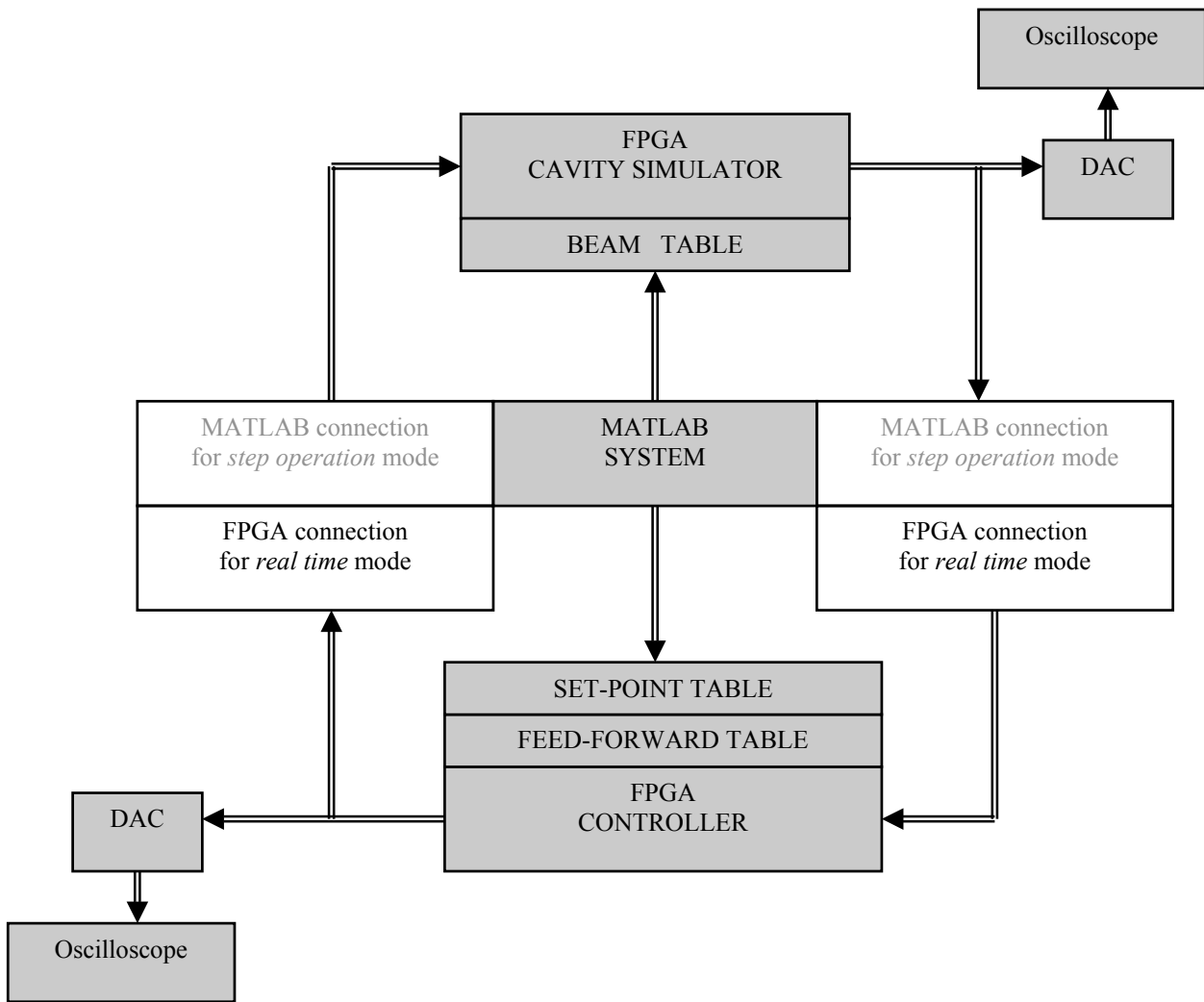


Figure 13. Functional diagram for one chip FPGA system.

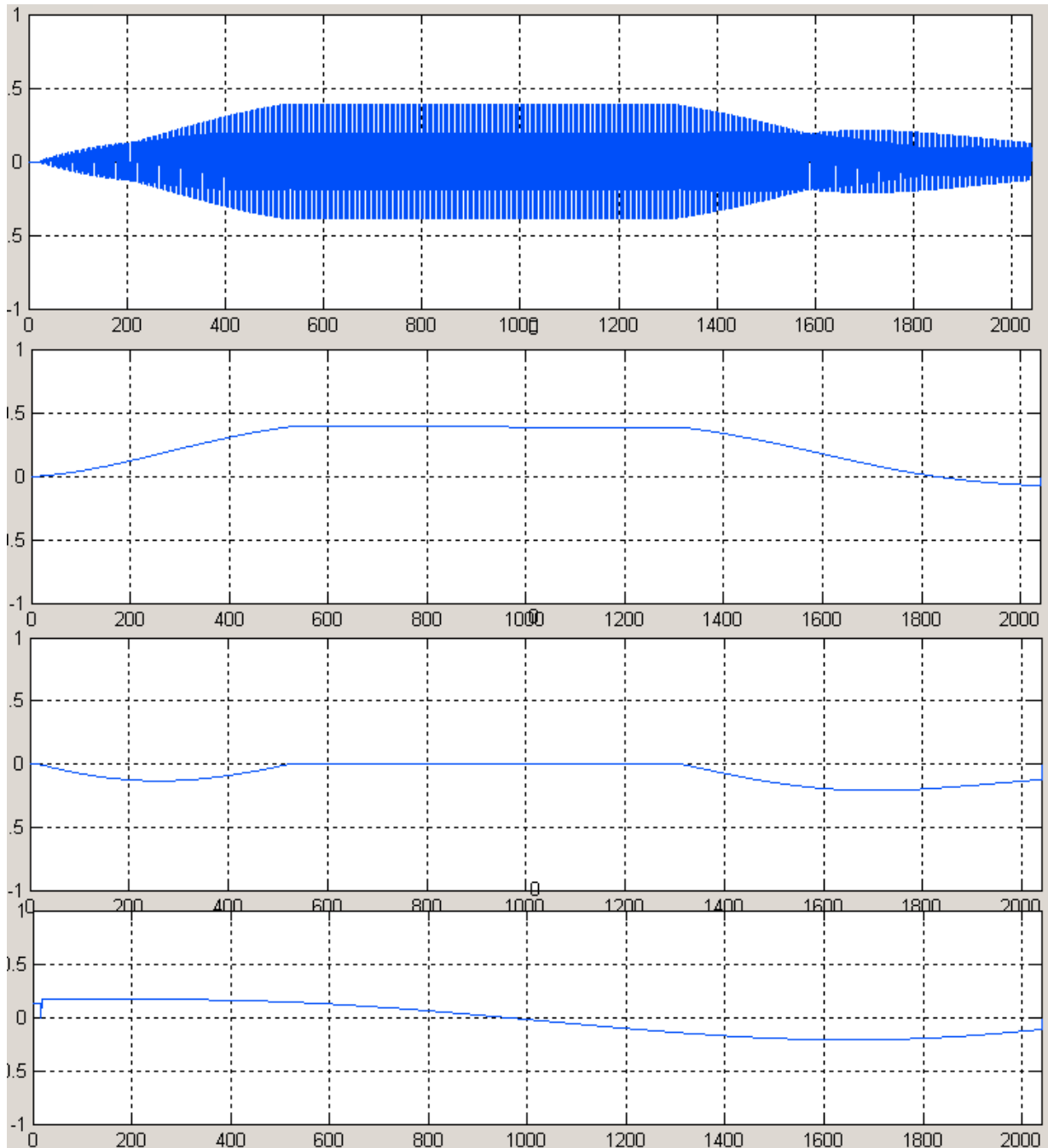


Figure. 14. Matlab windows recording data of FPGA cavity simulator output for real time one pulse operation.

From upper side: 1 - modulated signal of 250 kHz, 2 – I - component, 3 – Q - component, 4 - detuning.

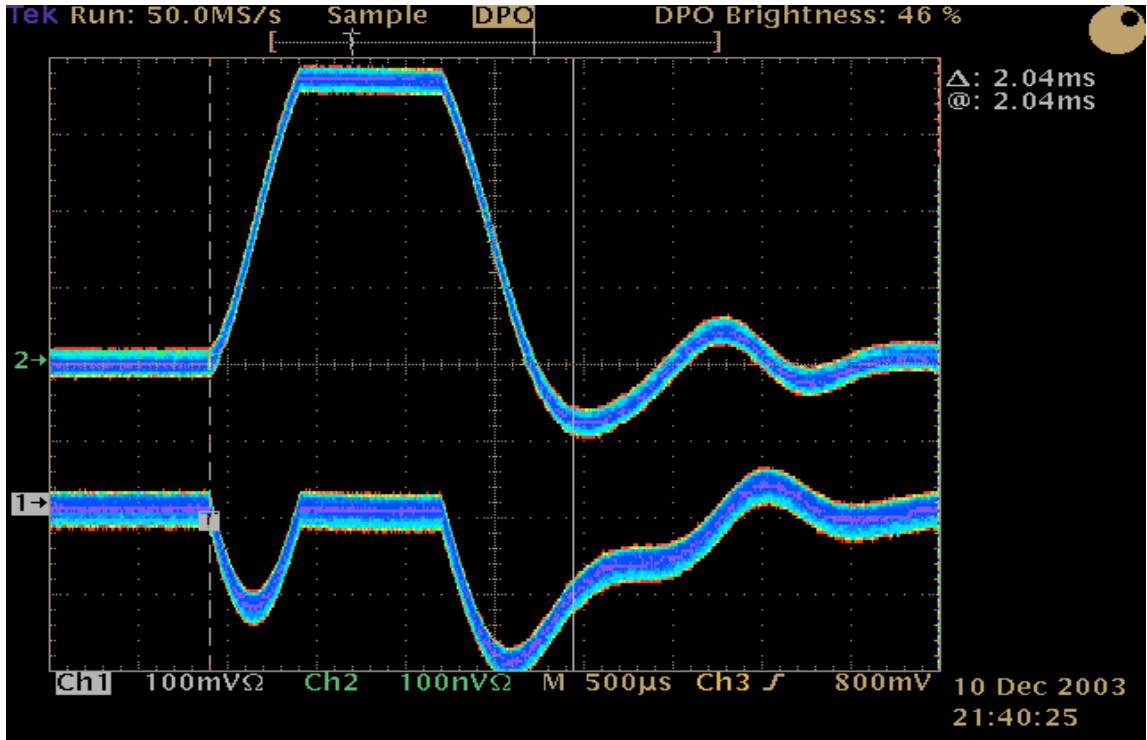


Figure 15. Oscilloscope picture (DPO mode) for cavity envelope: I and Q components.

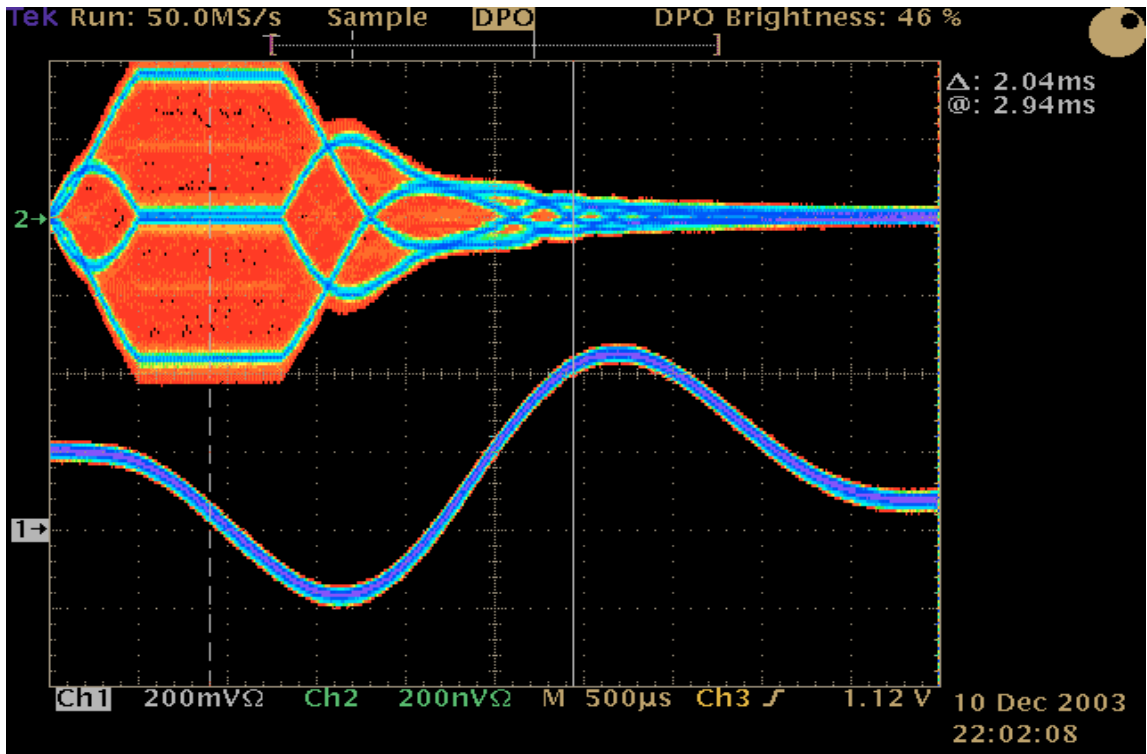


Figure 16. Oscilloscope picture (DPO mode) for cavity modulated signal and resultant detuning.

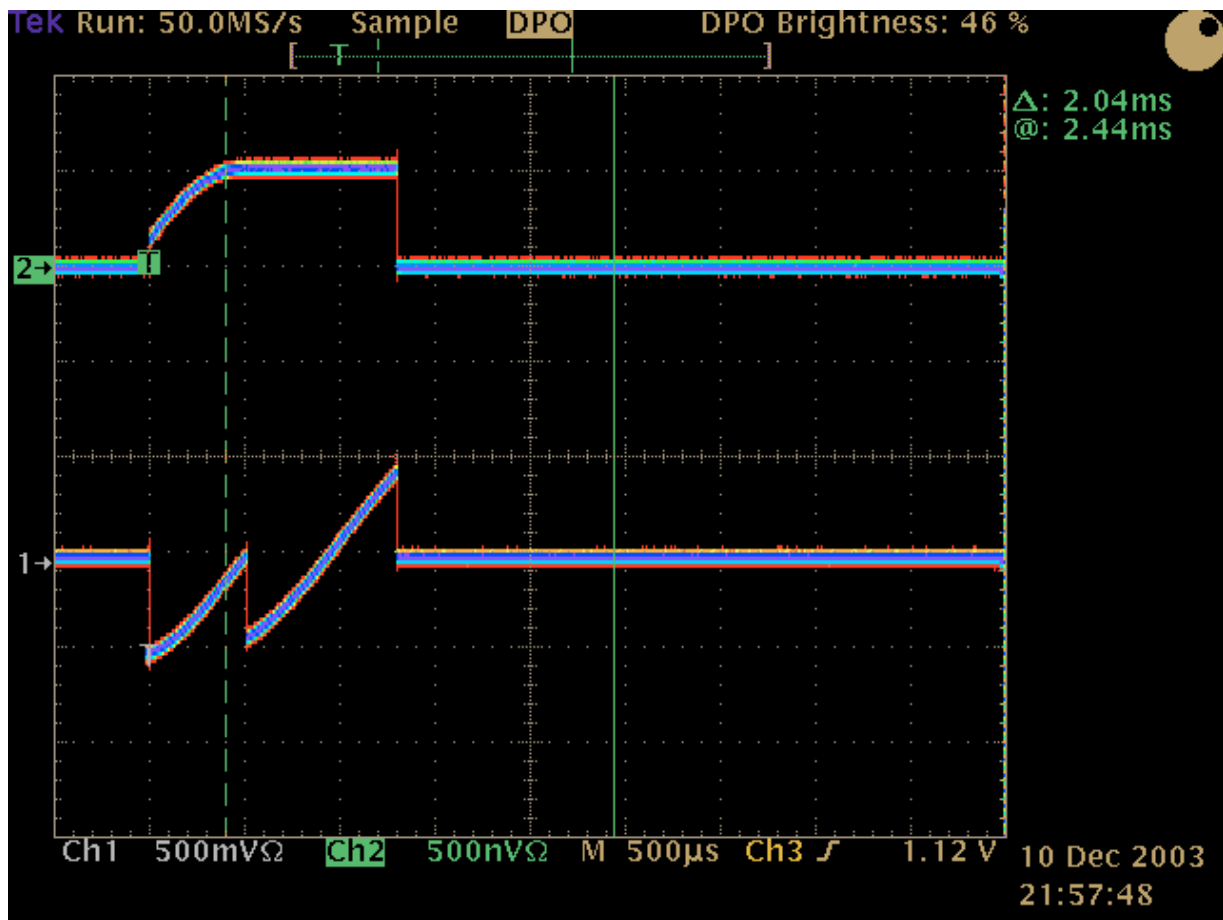


Figure 17. Oscilloscope picture (DPO mode) for controller output ( I and Q components) equal to cavity input.

## 5. CONCLUSION

The TESLA cavity simulator has been successfully implemented applying the very fast FPGA technology for the control system purpose. The efficient algorithm for the digital signal processing has concluded in the comprehensive cavity modeling. The proper parameters and variables scaling has provided the top potential numerical precision. The FPGA cavity simulator has been carefully investigated for different operational conditions. The step operation method has been proven as very efficient for the testing of the FPGA device coupled to the MATLAB system. The FPGA signal processing has been verified according to the required algorithm of the reference MATLAB cavity. The FPGA implementation with 18-bit resolution only is quite sufficient for the simulation purpose and the control system testing. The cavity simulator can be adopted for super-conductive and normal conductive resonators models applying diverse parameters.

The resources occupied by the 18-bit resolution model allows for very optimistic predictions concerning the simulation and control of numerable cavities by a single FPGA chip.

## REFERENCES

1. T. Schilcher, “*Vector Sum Control of Pulsed Accelerating Fields in Lorentz Force Detuned Superconducting Cavities*”, Ph. D. thesis, Hamburg, August 1998.
2. TESLA Technical Note, 2003-06:  
“*Cavity Control System Essential Modeling For TESLA Linear Accelerator*”. T. Czarski, R.S. Romaniuk, K.T. Pozniak - Warsaw University of Technology, S. Simrock – DESY.
3. TESLA Technical Note, 2003-08:  
“*Cavity Control System, Models Simulations For TESLA Linear Accelerator* ”. T. Czarski, R.S. Romaniuk, K.T. Pozniak - Warsaw University of Technology, S. Simrock – DESY.
4. TESLA Technical Note, 2003-09:  
*Cavity Control System, Advanced Modeling and Simulation for TESLA Linear Accelerator* - T. Czarski, R.S. Romaniuk, K.T. Pozniak - Warsaw University of Technology, S. Simrock – DESY.
5. TESLA Technical Note, 2003-22:  
*FPGA Based Cavity Simulator for TESLA Test Facility* - W.M. Zabolotny, T. Czarski, T. Jezynski, K.T. Pozniak, P. Rutkowski, R.S. Romaniuk - Warsaw University of Technology, K. Bunkowski - Warsaw University, S. Simrock – DESY.